Vol. 550: 83–99, 2016
doi: 10.3354/meps11700

MARINE ECOLOGY PROGRESS SERIES
Mar Ecol Prog Ser

Published May 25

# Building a model of ammonium excretion in two species of marine zooplankton based on glutamate dehydrogenase kinetics

**I. Fernández-Urruzola[1,*], N. Osma[1], M. Gómez[1], S. Montesdeoca-Esponda[2], T. T. Packard[1]**

[1]Marine Ecophysiology Group (EOMAR), Universidad de Las Palmas de Gran Canaria, 35017, Spain
[2]Environmental Chemical Analysis Group, Universidad de Las Palmas de Gran Canaria, 35017, Spain

ABSTRACT: $NH_4^+$ production in 2 species of marine zooplankton was predicted from glutamate dehydrogenase (GDH) activity using general bisubstrate enzyme kinetics during a period of starvation. In addition to starvation, we studied the effect of food quality on both $NH_4^+$ excretion rates ($RNH_4^+$) and the biochemical composition of zooplankton. The mathematical function used here relies on Michaelis-Menten principles and assumes that the synthesis of $NH_4^+$ is controlled mainly by the maximum velocity of GDH, the intracellular pool of substrates and the kinetic constants. This simple model described reasonably well the shifts in $RNH_4^+$ that occurred within the time course of starvation in both groups of zooplankton. The calculated $RNH_4^+$, however, underestimated the actual $RNH_4^+$. Furthermore, we used single substrate kinetics to address the magnitude of either the allosteric inhibition or the activation by purine nucleotides. We found that allosterism is more important in healthy physiological conditions. Overall, the use of first-principles kinetics seems to provide better estimates of $RNH_4^+$ than applying a general GDH/$RNH_4^+$ ratio on the measurements of GDH; therefore, its application may be of potential interest when studying zooplankton $RNH_4^+$ in heterogeneous marine ecosystems.

KEY WORDS: Glutamate dehydrogenase · $NH_4^+$ excretion · Biochemical kinetics · *Brachionus plicatilis* · *Leptomysis lingvura*



## INTRODUCTION

Most of the transformations of nitrogen that occur in the marine environment are controlled by a few enzymes. Among these, glutamate dehydrogenase (GDH) is of critical importance. It has been found in nearly every living organism and plays a major role in nitrogen metabolism. In the oxidative deamination reaction, $NAD(P)^+$-specific GDH (EC 1.4.1.3) feeds into the tricarboxilic acid (TCA) cycle by converting L-glutamate to α-ketoglutarate with the concominant reduction of $NAD(P)^+$ to NAD(P)H and by serving as the main pathway for $NH_4^+$ excretion in marine heterotrophs (Bidigare & King 1981). $NH_4^+$ is the primary nitrogen compound released by these organisms in the ocean water column (Regnault 1987, Steinberg & Saba 2008) and constitutes the most reduced form of nitrogen and, thereby, the most efficient in terms of assimilation. At a global scale, $NH_4^+$ regeneration satisfies about 80% of the phytoplankton requirements (Harrison 1992), which reflects the significance of this nitrogen source in the nutrient fluxes of epipelagic waters. In view of its metabolic role, the enzyme GDH has been routinely used in oceanographic research for the appraisal of $NH_4^+$ regeneration in marine ecosystems (e.g. Fernández-Urruzola et al. 2014). Such an enzymatic approach not only benefits from a high data aquisition rate, but also circumvents all the inherent constraints of classical methods (i.e. incubations). However, it requires a

*Corresponding author: ifernandez@becarios.ulpgc.es

substrate surplus to guarantee specificity of the reaction and reproducibility of the measurement (Maldonado et al. 2012). These saturating levels of substrates are unlikely *in vivo*, so actual $NH_4^+$ excretion rates ($RNH_4^+$) have to be inferred from potential measurements by applying an empirically determined factor that relates $RNH_4^+$ and GDH activities (i.e. the GDH/$RNH_4^+$ ratio). Unfortunately, their relationship is not universal, but may vary substantially depending on taxon, size and trophic condition, among other biological factors. This results in large uncertainties of up to 43% (Fernández-Urruzola 2016), i.e. inaccurate estimations of $RNH_4^+$, when using a single GDH/$RNH_4^+$ value to study heterogenous populations of zooplankton at sea.

Exploring the biochemical mechanisms of $NH_4^+$ production through the GDH reaction should provide knowledge on the intracellular processes that control it and, thereby, improve the predictions of $RNH_4^+$ based on GDH activities. Yet, few attempts have been made to relate metabolic rates such as $RNH_4^+$ to fundamental chemical principles. Despite their simplicity, biochemical models based on enzyme kinetics have rarely been utilized in biological oceanography studies. This was first noted by Packard et al. (1996), who investigated enzymatic control in the respiratory electron transport system (ETS) of a marine bacterium, and subsequently demonstrated that an enzyme kinetic model would provide better predictive capability of respiratory $O_2$ consumption rates than those models based on allometric equations relating respiration to body size (Aguiar-González et al. 2012). Nevertheless, these studies were mainly heuristic modeling exercises that calculated substrate concentrations from changes in carbon sources and bacterial biomass rather than by performing direct measurements of the intracellular levels of pyridine nucleotides. The kinetic constants, in turn, were taken from other organisms and optimized for their model through successive iterations. It was not until Roy & Packard (2001) that a kinetic model was built in a marine organism by incorporating newly measured kinetic constants and experimentally determined intracellular levels of isocitrate and $NADP^+$. These authors applied the same biochemical principles to the enzyme isocitrate dehydogenase in order to predict the rate of $CO_2$ production in the bacterium *Pseudomonas nautica*. This approach could also be extended to many other metabolic processes such as $N_2$ fixation, ATP production or, as in the case here, $NH_4^+$ excretion (Packard et al. 2004). All these processes are of major importance in biogeochemical cycles, so they should be quantified to characterize the metabolic state of marine ecosystems. In this sense, the kinetic models would constitute a suitable alternative for calculating physiological rates (e.g. $RNH_4^+$) when direct measurements are unfeasible.

A first-principles modeling approach could be designed to describe the mechanics of the GDH reaction in terms of how changes in metabolite concentrations affect the local $NH_4^+$ production rate. The rationale behind kinetic models is that each metabolic process is controlled by maximum velocity ($V_{max}$), substrate availability and equilibrium constants. Based on Michaelis-Menten as the fundamental equation, they assume the steady-state condition of the enzyme-substrate (ES) complex, i.e. $d[ES]/dt = 0$, which should be valid as long as the substrate concentration exceeds the enzyme concentration (Bisswanger 2008). This simple approach, however, is often complicated by the role of inhibitors and activators. In fact, the GDH reaction is allosterically regulated by enzyme modulators such as the purine nucleotides guanosine-5′-triphosphate (GTP) and adenosine-5′-diphosphate (ADP) (Frieden & Colman 1967). Furthermore, various authors reported substrate inhibition with either glutamate (Glu) or nicotinamide adenine dinucleotide ($NAD^+$) (Engel & Dalziel 1970, Barton & Fisher 1971), but at concentrations that are unlikely in living cells. Aside from allosteric effects, GDH has been proposed to follow a random sequential bi-bi mechanism in the Glu deamination reaction (Rife & Cleland 1980), meaning that there is no particular order in the sequential binding of any of the 2 substrates to the active site. Since substrate availability is the most obvious mechanism in enzyme regulation, in this study we assume these simple kinetics as the most appropriate to calculate the actual velocity of $NH_4^+$ production ($VNH_4^+$). The importance of GTP and ADP as allosteric modulators of GDH were not included in the bisubstrate model, but studied on a monosubstrate basis, since the kinetic equation would otherwise become too complex to achieve empirically.

In the present study, we aimed to demonstrate the shifts in $RNH_4^+$, GDH activities, as well as in the intracellular substrate (Glu and $NAD^+$) and effector (GTP and ADP) levels during a starvation time course, in 2 species of marine zooplankton (*Brachionus plicatilis* and *Leptomysis lingvura*). Using this demonstrated shift over the starvation time course, we tested the ability of the proposed kinetic model to predict changes in $RNH_4^+$ in response to environmental forcings. Although previous works (e.g. Packard et al. 1996, Roy & Packard 2001) focused on marine bacterium in order to reduce problems of organelle

organization and behavior, the same theoretical concept should work for metazoans (Packard & Gómez 2008). In this sense, we chose zooplankters of different structural complexity to study how it affects the accuracy of the model. Since the source of nitrogen may also cause a change in $RNH_4^+$ (Saba et al. 2009), we also address its influence on the excretory machinery by growing both organisms on 2 diets of different nutritional quality. The main goal of this study was thus to verify whether a kinetic modeling approach can provide better estimates of $RNH_4^+$ in a changing food environment than the classical approach based on a constant GDH/$RNH_4^+$ and the measurement of the GDH activity can.

## MATERIALS AND METHODS

### Cultures of marine organisms

Two species of marine zooplankton, the rotifer *Brachionus plicatilis* and the mysid *Leptomysis lingvura*, were used to test the ability of a GDH kinetic model in the prediction of $RNH_4^+$. Both organisms, as well as 2 of their prey species (the algae *Nannochloropsis* sp. and the crustacea *Artemia* sp.), were cultured under laboratory-controlled conditions. *B. plicatilis* were grown in 2 plastic tanks containing 20 l of diluted seawater (~23 PSU) at 25°C that was previously filtered through GF/F filters. These tanks were gently aerated to maintain saturating oxygen conditions and were kept in the dark. Solid removal by siphoning and water exchange were performed daily to prevent dissolved $NH_4^+$ concentrations above 0.1 mg $l^{-1}$. Rotifers were fed with 2 diets that differed substantially in fatty acid composition (Lubzens et al. 1995): one tank was provided with live microalgae *Nannochloropsis* sp. (ESD = 2–3 µm), rich in polyunsaturated fatty acids, at a concentration of $1.2 \times 10^5$ cells $rotifer^{-1}$ $d^{-1}$; the other tank was provided with a low-lipid diet consisting of 0.8 µg dry yeast $rotifer^{-1}$ $d^{-1}$. Food was supplied continuously through peristaltic pumps for each tank. Both treatments achieved (see Table 1) relatively high densities of about 200 rotifers $ml^{-1}$. Thus, it was necessary to grow *Nannochloropsis* sp., which were cultured in 8 l plastic carboys filled with autoclaved 0.2 µm filtered seawater and enriched with *f*/2 medium (Guillard 1975). Batch cultures of *Nannochloropsis* sp. were kept bubbled in a culture chamber at a constant temperature of 20°C and a light intensity of 54.1 µmol photons $m^{-2}$ $s^{-1}$ on a 16 h light:8 h dark cycle.

*L. lingvura* were collected at sea and immediately transferred to the culture system installed in the laboratory, which consisted of 12 glass aquariums (40 l each) suspended in a circulating water bath. Mysids were fed twice a day with 2 diets that, again, were characterized by their different nutritional qualities (Table 1): *Artemia* sp. nauplii, lipid-enriched with Easy-DHA Selco® (INVE) and harvested after 48 h were provided at a concentration of 100 *Artemia* $mysid^{-1}$ $d^{-1}$; the second diet, poor in lipids, consisted of 400 rotifers (*B. plicatilis*) $mysid^{-1}$ $d^{-1}$ from the aforementioned yeast-grown culture. According to Domingues et al. (2000), those food concentrations would satisfy the mysid's demands.

### Experimental procedure

Both *B. plicatilis* and *L. lingvura* were acclimated to each feeding treatment for 1 wk before experimentation. Afterwards, the organisms were assayed, after feeding ad libitum on each diet, in order to measure $RNH_4^+$ and the associated biochemistry during well-fed conditions ($t_0$). $RNH_4^+$ was measured using water-bottle incubations; after each experiment, the zooplankters were frozen in liquid N (–196°C) and stored at –80°C for subsequent analyses of GDH activities, the kinetic constants and the concentrations of those metabolites involved in the catabolism of Glu (Glu, $NAD^+$, ADP, GTP). For statistical strength, we performed several replicates at $t_0$. Then, rotifers were harvested and deposited in new tanks containing 0.2 µm filtered seawater. Mysids were

Table 1. Culture conditions for *Brachionus plicatilis* and *Leptomysis lingvura*. Food levels were maintained for 1 wk prior to experimentation and at $t_0$. The same food levels were provided again after starvation experiments (i.e. after 28 and 60 h of starvation for *B. plicatilis* and *L. lingvura*, respectively)

| Temp. (°C) | Salinity (PSU) | Day:night cycle (h) | Lipid-rich diet | Lipid-poor diet |
|---|---|---|---|---|
| ***B. plicatilis*** | | | | |
| 25 | 23 | 16:08 | *Nannochloropsis* sp. ($1.2 \times 10^5$ cells $rotifer^{-1}$ $d^{-1}$) | Dry yeast (0.8 µg $rotifer^{-1}$ $d^{-1}$) |
| ***L. lingvura*** | | | | |
| 18 | 35 | 14:10 | Enriched *Artemia* sp. (100 *Artemia* $mysid^{-1}$ $d^{-1}$) | Yeast-grown *B. plicatilis* (400 rotifers $mysid^{-1}$ $d^{-1}$) |

likewise moved into new aquariums filled with 0.2 µm filtered seawater. No food was provided to these tanks, so that rotifers and mysids starved for 28 and 60 h, respectively. Accordingly, there were shifts in the morphology of these organisms with starvation; in addition, egg production decreased dramatically in both species. Over the entire period, we performed continuous seawater exchanges to avoid high bacterial concentrations, which could contribute to the rotifer's nutrition. These periods of starvation were set in accordance to Kirk (1997), who found a mean starvation survival of about 2 d for various species of rotifers. Similarly, Fernández-Urruzola et al. (2011) observed increased mortality in starved mysids after 68 h. Throughout all this time, organisms were assayed for $R\mathrm{NH_4^+}$, at time-intervals from 2 to 12 h. Afterwards, pulses of food were given to the zooplankters in order to test if any recovery in either the physiological and biochemical rates occurred.

### Water-bottle incubations

Organisms were washed twice in filtered seawater before experimentation. To ensure homogeneity in the rotifer samples, we conducted a size-selective harvest by using a 100 µm mesh. For mysids, adults were selected for experimentation. Organisms were carefully added to 60 ml gas-tight glass bottles by siphoning. Densities were similar in each bottle and experimental session in order to avoid methodological biases in $R\mathrm{NH_4^+}$ as a result of overcrowding: *B. plicatilis* were incubated at concentrations of 500–550 rotifers $\mathrm{ml^{-1}}$, while *L. lingvura* were incubated at concentrations of 6–8 mysids $\mathrm{bottle^{-1}}$ depending on their size. Individuals were alive in all cases after experimentation. All the experiments were conducted in triplicate and included at least 2 control flasks without organisms. Furthermore, dissolved oxygen was measured in each bottle with continuously installed oxygen electrodes (Strathkelvin 928 Oxygen System® respirometer). This allowed exploration of changes in the respiration ($R\mathrm{O_2}$) to $R\mathrm{NH_4^+}$ relationship. Incubations were maintained in the dark to avoid any autotrophic activity, and lasted 1–1.5 h at culturing temperature. Such short incubation times ensured linear $R\mathrm{NH_4^+}$ during the experiment (Fig. 1). Then, 10 ml of seawater was siphoned off each bottle for $\mathrm{NH_4^+}$ determinations according to the Holmes et al. (1999) method. Organisms were frozen in liquid nitrogen and stored at –80 °C for subsequent enzymatic analyses.

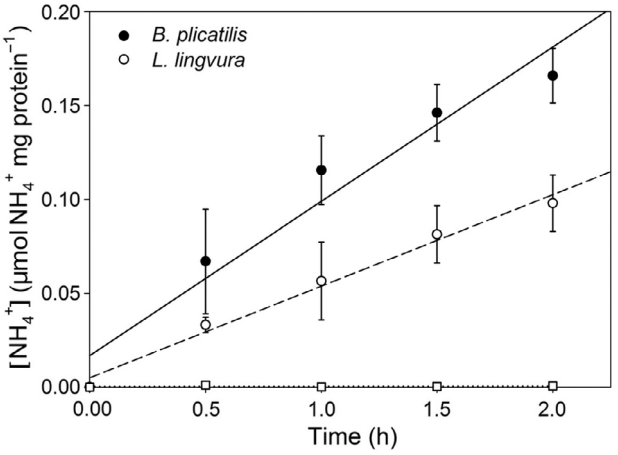


Fig. 1. *Brachionus plicatilis*, *Leptomysis lingvura*. Increase in $\mathrm{NH_4^+}$ concentration with incubation time. Squares and dotted line represent blanks. Error bars: 95% confidence intervals

### Measurements of GDH activity

Samples were thawed and then sonicated in Tris medium (0.1 mM, pH = 8.6). Aliquots of the homogenate were immediately frozen at –80°C for the eventual quantification of protein content, and the intracellular levels of Glu, $\mathrm{NAD^+}$, ADP and GTP. The remainder was centrifuged for 8 min at 1500 × *g* at 0°C, and the resultant supernatant fluid was assayed for GDH activity. The whole process was performed at 0–4°C and did not exceed 30 min in order to preclude any loss of activity. The GDH assay was run according to Bidigare & King (1981), using fluorometry as introduced by Fernández-Urruzola et al. (2011). We added saturating levels of substrates (50 mM Glu and 1.2 mM $\mathrm{NAD^+}$), as well as 2 mM of ADP to avoid any possible inhibition caused by GTP molecules. The increasing fluorescence signal of NADH was monitored for 4 min. The regression line of NADH production with time (the slope) was used to calculate the GDH activity using a standard curve generated with known concentrations of pure GDH (EC 1.4.1.3).

### Kinetic constants

Some samples were chosen to evaluate the kinetic constants of GDH. As postulated by Rife & Cleland (1980), we assumed the steady-state random sequential bi-bi mechanism, which is valid as long as the product is negligible (Bisswanger 2008). The corresponding Michaelis-Menten equation reads in the form:

$$V\mathrm{NH_4^+} = \frac{V_{max}\ [\mathrm{Glu}][\mathrm{NAD^+}]}{K_{ia}K_{NAD} + K_{NAD}[\mathrm{Glu}] + K_{Glu}\ [\mathrm{NAD^+}] + [\mathrm{Glu}][\mathrm{NAD^+}]} \quad (1)$$

where $V\mathrm{NH_4^+}$ is the actual rate of $\mathrm{NH_4^+}$ production (*in vivo*), $V_{max}$ is the apparent maximum enzyme reaction rate, $K_{ia}$ is the dissociation constant associated with the first binding substrate (i.e. Glu) and $K_{Glu}$ and $K_{NAD}$ are the Michaelis half-saturation constants $K_m$ for Glu and $\mathrm{NAD^+}$, respectively.

Kinetic parameters were measured with 5 different concentrations of Glu (0.4, 2, 10, 40 and 60 mM) and $\mathrm{NAD^+}$ (0.05, 0.2, 0.6, 1.2 and 2 mM), leading to a 5 × 5 data matrix. These substrate concentrations were set according to Bisswanger (2011), who suggests a range starting 1 order of magnitude below and ending 1 order of magnitude above each $K_m$. The approximate $K_m$ values were already known from preliminary investigations (Fernández-Urruzola et al. 2011). Furthermore, measurement of all combinations in the matrix (25) allowed a compromise with the stability of the enzyme, since each homogenate was assayed for <1 h in a spectrofluorometer equipped with a 4-cell holder. Changes in kinetic constants with starvation were tested by analyzing several replicates at $t_0$, a few hours after feeding and at the end of the experimental period.

The hyperbolic curves that resulted from varying Glu concentrations at different constant amounts of $\mathrm{NAD^+}$, and vice versa, became linear on applying double-reciprocal transformation (Lineweaver & Burk 1934). Accordingly, primary plots were constructed for each substrate by plotting their inverse concentrations (*x*-axis, 1/[Glu] and 1/[$\mathrm{NAD^+}$]) against the inverse of velocity (*y*-axis, 1/*v*; see Fig. 2a). All lines met at a common intercept left of the ordinate, which confirmed the proposed sequential reaction mechanism of GDH. Both the resultant slopes and *y*-intercepts from these primary plots of either substrate (e.g. 1/[$\mathrm{NAD^+}$]) were plotted in a secondary plot against the inverse of the other substrate (in this case, 1/[Glu]). The regressions of both slopes and intercepts also resulted in straight lines that cut the abscissa at $-1/K_{ia}$ and at $-1/K_{Glu}$, respectively (Bisswanger 2008). The same parameters were deducted for the cosubstrate ($\mathrm{NAD^+}$) by simply changing the order of the substrates plotted in the primary and secondary plots.

Additionally, the allosteric effect of purine nucleotides on GDH activity was studied. GTP and ADP are known to be an inhibitor and activator of the

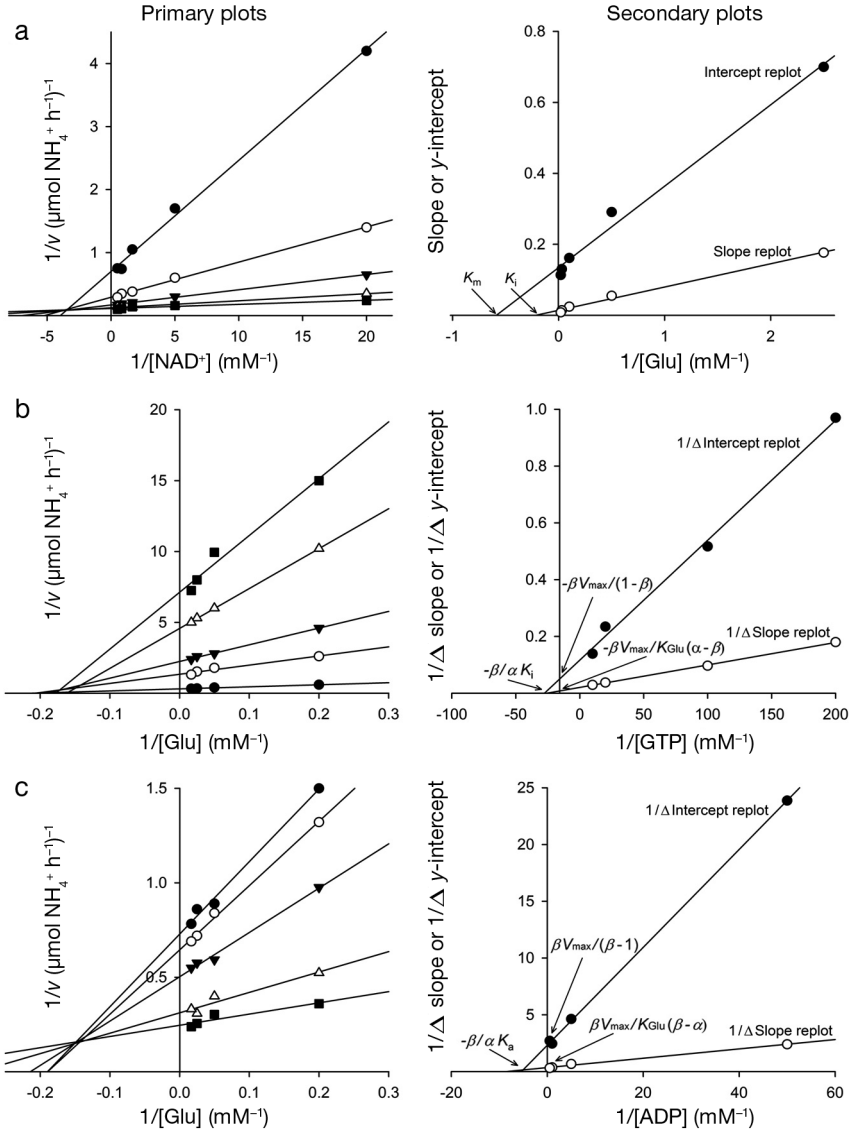


Fig. 2. Double-reciprocal representations (primary plots) of Michaelis-Menten equations for (a) a bi-bi random mechanism, (b) hyperbolic mixed-type inhibition and (c) non-essential activation. 1/v (*y*-axes on primary plots) stands for the inverse of the GDH reaction rate. Kinetic constants were determined from corresponding secondary plots, where 1/Δ refers to the inverse of the differences between either the slopes or intercepts plotted in the primary plots. All calculations are described in 'Materials and methods: Kinetic constants'

enzyme reaction, respectively (Frieden & Colman 1967). Their role in modulating GDH activity is demonstrated in Fig. 3. There is a specific binding site for these molecules, which means that they do not compete with substrates for binding to the active site. The enzyme–substrate (ES) complex is not linearly inhibited by GTP, i.e. infinite GTP concentrations reduce, but do not completely eliminate, enzyme reaction activity (see Fig. 3). The same holds true for activation by ADP. Accordingly, there is a hyperbolic mixed inhibition, where both $V_{max}$ and $K_{Glu}$ (considering Glu as the first binding substrate) are affected by effector concentrations. These changes in $V_{max}$ and $K_{Glu}$ with effector molecules will be described by the factors α and β, respectively. In the simplest case study of monosubstrate reactions, the general Henri-Michaelis-Menten form of the velocity for this type of inhibition should read as follows (Segel 1993):

$$VNH_4^+ = \frac{V_{max}[Glu]}{K_{Glu}\left(1 + \frac{[GTP]}{K_{i_{slope}}}\right) + [Glu]\left(1 + \frac{[GTP]}{K_{i_{int}}}\right)} \quad (2)$$

where $K_{i_{slope}}$ refers to the apparent $K_i$ value that accounts for the change in the slope of the reciprocal plot,

$$K_{i_{slope}} = \frac{\beta_i[GTP] + \alpha_i K_i}{(\alpha_i - \beta_i)} \quad (3)$$

and $K_{i_{int}}$ refers to the apparent $K_i$ value calculated from the 1/$v$-axis intercept:

$$K_{i_{int}} = \frac{\beta_i[GTP] + \alpha_i K_i}{(1 - \beta_i)} \quad (4)$$

The same concept should be applied for the ADP activation study:

$$VNH_4^+ = \frac{V_{max}\ [Glu]}{K_{Glu}\frac{\left(1 + \frac{[ADP]}{K_a}\right)}{\left(1 + \frac{\beta\ [ADP]}{\alpha K_a}\right)} + [Glu]\frac{\left(1 + \frac{[ADP]}{\alpha\ K_a}\right)}{\left(1 + \frac{\beta\ [ADP]}{\alpha K_a}\right)}} \quad (5)$$

To derive all these inhibition constants, we followed a similar procedure to the one described above for bisubstrate kinetics. We plotted GDH activities at different concentrations (0.2, 1, 5, 20, 40 and 60 mM) of the first binding substrate (i.e. Glu), each measured at different constant amounts of GTP (0, 5, 10, 50 and 100 µM) or ADP (0, 0.02, 0.2, 1 and 2 mM). The hyperbolic curves were then linearized through a reciprocal transformation (Fig. 2b,c). The inverse concentrations of Glu ($x$-axis, 1/[Glu]) were plotted in a primary plot against the inverse of the velocity ($y$-axis, 1/$v$). Plotting the resultant slopes and intercepts against the concentrations of the effector would still result in hyperbolas; therefore, it was necessary to apply a differential method to achieve linearization. The inverse of either Δintercepts or Δslopes was represented in a secondary plot against the inverse of the effector concentration ($x$-axis). Δ is the difference between the value at a given concentration of inhibitor and the value at zero inhibitor concentration (and vice versa in the activation case study). The kinetic parameter β, either for inhibition ($\beta_i$) or activation ($\beta_a$), was calculated from the ordinate intercept in the 1/Δ intercept replot as follows:

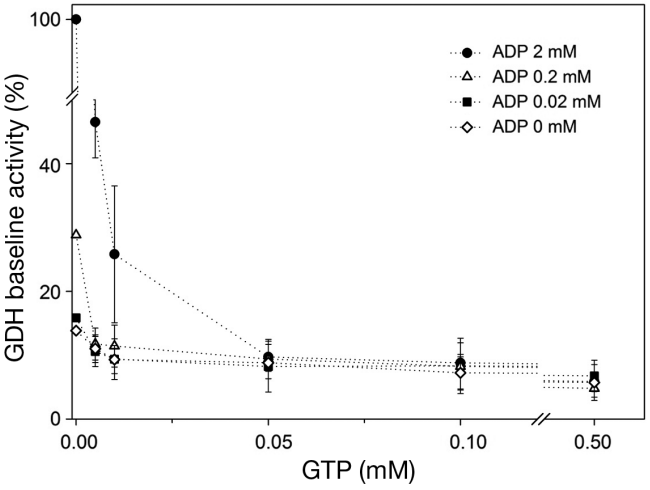


Fig. 3. GTP inhibition of GDH activity in the direction of glutamate deamination, at different levels of ADP. Error bars: 95% confidence intervals

$$\beta_i = \frac{Intercept}{K_{Glu}Intercept},\ \beta_a = \frac{Intercept}{Intercept - V_{max}} \quad (6)$$

and α, either for inhibition ($\alpha_i$) or activation ($\alpha_a$), was determined from the ordinate intercept in the 1/Δslope replot:

$$\alpha_i = \frac{\beta_i V_{max}}{K_{Glu}Intercept} + \beta_i \qquad \alpha_a = \beta_a - \frac{\beta_a V_{max}}{K_{Glu}Intercept} \quad (7)$$

$V_{max}$ and $K_{Glu}$ were obtained from the ordinate and abscissa intercepts of the control line (i.e. at zero effector concentration) from the primary plot. Knowing α and β, one can calculate $K_i$ and $K_a$ for both Δslope and Δintercept replots through Eq. (8):

$$K_i = \frac{\beta_i slope}{\alpha_i Intercept} \qquad K_a = \frac{\beta_a slope}{\alpha_a Intercept} \quad (8)$$

### Intracellular levels of metabolites

**Glutamate.** Levels of intracellular glutamate were measured using the method described by Hans-Otto & Michal (1974). It uses the GDH reaction to deaminate all intracellular free glutamate; the resultant NADH is then oxidized in a second reaction and catalyzed by the diaphorase, where it donates electrons to the tetrazolium chloride dye, INT (2-p-iodophenyl-3-p-nitrophenyl), to form formazan. The absorbance of this latter molecule was spectrophotometrically measured at 492 nm and stoichiometrically related to the free glutamate concentration ([Glu]) through Eq. (9):

$$[\mathrm{Glu}] = \frac{Vol\ MW_{\mathrm{Glu}}}{\varepsilon\ l\ vol \times 1000} \times \Delta\mathrm{Glu} \qquad (9)$$

where *Vol* is the total volume of the reaction mixture, $MW_{\mathrm{Glu}}$ is the molecular weight of glutamate, ε is the extinction coefficient of INT, *l* is the cuvette light-path and *vol* is the subsampled homogenate volume. ΔGlu stands for the difference between the absorbance before adding GDH to the reaction mixture and the absorbance at the reaction end-point, both corrected by a control measure with MilliQ water instead of subsample homogenate.

**Pyridine nucleotide: $NAD^+$.** Levels were determined using the enzymatic cycling system described in Wagner & Scott (1994), with small modifications. This method allows amplification of the signal by coupling 3 serial reactions. Samples were centrifuged as described above. The supernatant was then assayed distinguishing between the oxidized ($NAD^+$) and reduced (NADH) forms by means of heat (30 min at 60°C), which destroys the oxidized forms without affecting the reduced ones. Accordingly, the difference between the total pool of this pyridine nucleotide ($NAD_t$) and the pool of its reduced form would result in the intracellular levels of $NAD^+$.

A volume of either the heated or unheated extracts (100 µl) was added to 800 µl of ice-cold freshly prepared NAD cycling buffer (100 mM Tris-HCl buffer with 1% bovine serum albumin, pH = 8.0) and incubated in the dark at 37°C for 5 min. The enzyme cycling system uses 0.2 mg $ml^{-1}$ of the enzyme alcohol deshydrogenase (ADH) and a non-enzymatic reaction to cycle $NAD^+$ between its oxidized and reduced forms in the presence of ethanol (100 µl) and 1 mM phenazine ethosulfate (PES). PES reduces 0.5 mM thiazolyl blue (MTT) into its formazan in another non-enzymatic reaction. Before spectrophotometrically measuring the MTT–formazan production, a quick centrifugation (16 000 × *g*, 30 s) was performed to remove any insoluble material. Afterwards, the change in absorbance at 570 nm was monitored over 3 min at 37°C in a thermostated multi-cell holder attached to a refrigerated recirculator.

**Phosphate nucleotides: GTP and ADP.** For the determination of the intracellular concentrations of ADP and GTP we employed a Varian Prostar chromatographic system (Varian). It consisted of a pump, an autosampler, a column valve module with an internal oven and a diode array detector working at 254 nm. The 2 analytes were separated on a PRP-1 column (5 µm, 2.1 × 150 mm; Hamilton), applying a column temperature of 50°C. Mobile Phase A was 100 mM monopotassium phosphate (adjusted pH to 7 with potassium hydroxide), 1 mM tetrabutylammmonium phosphate and 2.5% methanol. Mobile Phase B was Eluent A and 20% methanol. Elution was performed with a gradient that initially consisted of 1% of Mobile Phase B. It was maintained up to 3 min and then raised to 15% in 10 min, to 55% in 15 min, to 95% in 16 min and to 99% in 20 min (see Fig. 4). At 25 min the gradient returned to 1% of Mobile Phase B and was retained at that level for 5 min in order to equilibrate the column for the next injection. The flow rate was set to 0.3 ml $min^{-1}$, and the injection volume was 10 µl.

Stock solutions of each compound (1.42 mM) were prepared by dissolving appropriate amounts of commercial products in the mobile phase, and were stored in glass-stoppered bottles at 4°C. Concentration curves were constructed in the range of 0.01–50 µM. In all cases, correlation coefficients were ≥0.992. The limits of quantification (LOQs) were calculated as the concentration at which a signal-to-noise ratio was ≥10. They were 0.0005 µM for GTP and 0.002 µM for ADP. To evaluate the precision, expressed as relative standard deviation (% RSD),

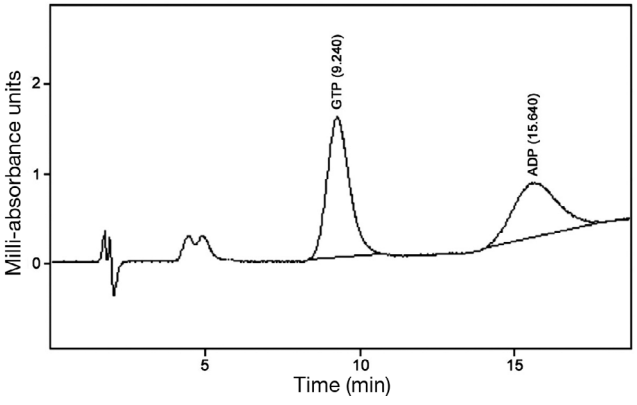


Fig. 4. Chromatogram for the phosphate nucleotides GTP and ADP from zooplankton samples, using UHPLC coupled to a diode array detector at 254 nm

6 replicate samples at 2 concentration levels (0.1 and 10 µM) were analyzed. The repeatability values obtained were, in both cases, <9%.

### Biomass and biovolume determinations

Protein content of each sample was determined as a measure of biomass by the method of Lowry et al. (1951) modified by Rutter (1967). Bovine serum albumin (BSA) was used as a standard. Each data point represented the mean of triplicate analyses.

In order to apply kinetic equations, the intracellular metabolites were given in terms of biovolume (i.e. molar units). Rotifer biovolume was calculated from protein content by a multiplying factor of 0.11 µg protein rotifer$^{-1}$ (±0.04, n = 30), and assuming a rotifer biovolume of $1.36 \times 10^6$ µm$^3$ after Boraas & Bennett (1988). Mysid biovolume was calculated using the equation $N\,(\mathrm{mg}) = 0.0546 + 0.0137\ Vol\,(\mathrm{mm}^3)$ given in Alcaraz et al. (2003), and a protein to N conversion factor of 0.521 (Postel et al. 2000).

## RESULTS

### Effect of diet on $NH_4^+$ excretory metabolism

In general, the response of $R\mathrm{NH_4^+}$, GDH activities and intracellular levels of Glu, $NAD^+$, GTP and ADP to different food qualities was more remarkable in *Brachionus plicatilis* than in *Leptomysis lingvura* (Table 2). Thus, $R\mathrm{NH_4^+}$ in *B. plicatilis* increased from 0.13 to 0.20 µmol $NH_4^+$ mg protein$^{-1}$ h$^{-1}$ when feeding on a more proteinaceous diet (i.e. yeast). This was not the case in *L. lingvura*, with $R\mathrm{NH_4^+}$ ranging between 0.08 and 0.09 µmol $NH_4^+$ mg protein$^{-1}$ h$^{-1}$. Accordingly, the $R\mathrm{NH_4^+}$ per mg protein of rotifers doubled that measured for mysids when exposed to such a dietary shift. As shown in Fig. 1, these rates were nearly constant over the experimental period (1–1.5 h). Longer incubation times (>1.5 h), however, induced a depression in $R\mathrm{NH_4^+}$, especially in *B. plicatilis*. On the other hand, the higher the lipid content in the diet, the higher the $R\mathrm{O_2}/R\mathrm{NH_4^+}$ ratios were. This was more noteable in *B. plicatilis*, so that those rotifers grown on the lipid-rich microalgae *Nannochloropsis* sp. had a maximum $R\mathrm{O_2}/R\mathrm{NH_4^+}$ ratio of 15.4. The same occurred in the mysids fed with the lipid-rich diet ($R\mathrm{O_2}/R\mathrm{NH_4^+}$ = 7.66), even though the difference with the correspondent value from those mysids fed with rotifers, poor in lipids, was not significant ($p > 0.05$). Similar to $R\mathrm{NH_4^+}$, the protein-specific GDH activities were higher for *B. plicatilis*. These potential enzymatic rates followed the same trends observed in $R\mathrm{NH_4^+}$. They peaked in the yeast-grown rotifers (2.21 µmol $NH_4^+$ mg protein$^{-1}$ h$^{-1}$). However, the differences in the GDH activities between the 2 treatments of *L. lingvura* were not so marked. All these trends in $R\mathrm{NH_4^+}$ and in enzymatic rates led to different GDH/$R\mathrm{NH_4^+}$ ratios, depending on the organism and the diet. They ranged from 11.05 to 14.69 in the rotifers and from 17.25 to 19.00 in mysids. Overall, ratios were slightly higher in those treatments consisting of the lipid-rich diet.

Regarding the intracellular levels of the metabolites, the differences between treatments were minimal (Table 2). Differences were more evident, how-

Table 2. Comparison of $R\mathrm{NH_4^+}$, GDH activitiy, $R\mathrm{O_2}/R\mathrm{NH_4^+}$ and GDH/$R\mathrm{NH_4^+}$ ratios, as well as intracellular levels of glutamate and other metabolites ($NAD^+$, GTP and ADP) in rotifers (*Brachionus plicatilis*) and mysids (*Leptomysis lingvura*) acclimated to 2 different types of diets (see Table 1). Data represent mean values ± SD, with the number of replicates in parentheses. Student's *t*-test was applied to study statistical differences for each parameter. Significant at $^*p < 0.05$, $^{**}p < 0.001$, $^{***}p < 0.0001$, ns: not significant ($p > 0.05$)

| | *Brachionus plicatilis* | | | *Leptomysis lingvura* | | |
|---|---|---|---|---|---|---|
| | Lipid-rich diet | Lipid-poor diet | p | Lipid-rich diet | Lipid-poor diet | p |
| $R\mathrm{NH_4^+}$ (µmol $NH_4^+$ mg protein$^{-1}$ h$^{-1}$) | 0.13 ± 0.04 (16) | 0.20 ± 0.06 (16) | *** | 0.09 ± 0.01 (8) | 0.08 ± 0.01 (8) | ns |
| $R\mathrm{O_2}/R\mathrm{NH_4^+}$ (molar basis)[a] | 15.38 ± 5.72 (16) | 8.75 ± 2.76 (16) | *** | 7.66 ± 2.48 (8) | 6.50 ± 2.90 (8) | ns |
| GDH activity (µmol $NH_4^+$ mg protein$^{-1}$ h$^{-1}$) | 1.91 ± 0.35 (16) | 2.21 ± 0.13 (16) | ** | 1.56 ± 0.10 (8) | 1.34 ± 0.11 (8) | * |
| GDH/$R\mathrm{NH_4^+}$ | 14.69 ± 5.25 (16) | 11.05 ± 3.37 (16) | * | 19.00 ± 3.94 (8) | 17.25 ± 2.85 (8) | ns |
| Glutamate (mM) | 6.49 ± 1.58 (16) | 7.27 ± 1.34 (16) | ns | 2.94 ± 0.45 (8) | 2.52 ± 0.52 (8) | ns |
| $NAD^+$ (µM) | 1.73 ± 0.34 (2) | 3.36 ± 1.57 (2) | ns | 3.89 ± 1.33 (8) | 4.50 ± 0.40 (8) | ns |
| GTP (mM) | 0.38 ± 0.07 (16) | 0.27 ± 0.05 (16) | *** | 0.16 ± 0.04 (8) | 0.15 ± 0.06 (8) | ns |
| ADP (µM) | 93.19 ± 33.41 (5) | 89.59 ± 32.00 (5) | ns | 16.85 ± 5.71 (8) | 17.70 ± 2.02 (8) | ns |

[a]Respiration data from Osma (2016)

ever, when organisms were compared. Except for $NAD^+$, *B. plicatilis* had 2- to 3-fold more Glu and GTP than *L. lingvura*. More specifically, the intracellular glutamate trends in the 2 zooplankters coincided with those described for their $RNH_4^+$. The differences in the metabolite concentrations become larger in the case of ADP, which was ~6 times higher in *B. plicatilis*.

### General kinetics of GDH during starvation

Despite the differences described above for all the variables considered in testing the general kinetic models of GDH, the 2 food treatments in both rotifers and mysids followed similar patterns with starvation (Fig. 5). In general, the maximum values of both $RNH_4^+$ and GDH activities were found at $t_0$, i.e. under well-fed conditions. This also describes the patterns of Glu, $NAD^+$, GTP and ADP. Afterwards, during the next 12 h, $RNH_4^+$, as well as metabolite concentrations, decreased sharply by half. GDH activities, however, declined more gradually during the time course. Furthermore, the decrease in enzymatic rates was more appreciable in the lipid-poor treatments than in the lipid-rich ones. In fact, the latter seemed to maintain relatively constant GDH activities over the experimental period. Except for GDH activities, all other variables responded to re-feeding (see vertical dotted lines in Fig. 5) by recuperating and even surpassing their initial values at $t_0$. This is especially clear in the case of $RNH_4^+$ and the substrates Glu and $NAD^+$.

The kinetic constants during both well-fed and starved conditions for each zooplankter were calculated following the procedures explained in the 'Materials and methods: Kinetic constants' section and illustrated in Fig. 2. Overall, $K_m$ values were lower in rotifers than in mysids (Table 3), especially in the case of $K_{Glu}$, which was about an order of magnitude smaller (0.12–0.49 mM). This means that the affinity of GDH for glutamate is higher in rotifers. $K_{NAD}$, however, was similar in the 2 species (ranging from 0.009 to 0.025 mM). Accordingly, $K_{NAD}$ was 1 to 2 orders of magnitude smaller than $K_{Glu}$ depending on the organism, but so were the intracellular levels of $NAD^+$ compared to those of Glu (Fig. 5). On the other hand, $K_{Glu}$ values increased slightly with starvation. Contrary to $K_m$, the $K_{ia}$ values of both Glu and $NAD^+$ were higher in rotifers than in mysids (Table 3). In this case, the higher the $K_{ia}$, the weaker the binding between the enzyme and the substrate. This also occurred when organisms starved, as $K_{ia}$ values increased significantly during food deprivation. Thus, both $K_{ia}$ and $K_m$ showed similar patterns when varying food availability, indicating a reduced reaction rate during starvation. Conversely, the inhibition ($K_i$) and activation ($K_a$) constants for GTP and ADP, respectively, seemed to remain relatively constant throughout the different feeding conditions. $K_i$ varied from $5.8 \times 10^{-4}$ to $6.0 \times 10^{-4}$ mM in *B. plicatilis* and from $1.7 \times 10^{-3}$ to $2.0 \times 10^{-3}$ mM in *L. lingvura*. $K_a$, in turn, ranged between 3.6 and 4.1 mM in *B. plicatilis* and between 0.7 and 5.8 mM in *L. lingvura*. Despite the wide range in the latter case, the high deviation could explain most of the variability.

Other factors to consider when studying either inhibition or activation of enzymatic rates are α and β. The factor α determines how $K_m$ of the substrate changes when the effector is bound to the enzyme; on the other hand, β is the factor by which $V_{max}$ changes when the effector occupies the enzyme. In the inhibition case study, α was between 1 and >1 in both rotifers (2.05–4.13) and mysids (2.50–5.04) and peaked during starvation (Table 3). The factor β, however, ranged between 0 and 1. It was significantly lower in rotifers (0.03–0.04) than in mysids (0.12–0.16). The opposite occurred with the factors α and β for activation. As expected, α was several times lower than β (Table 3).

All these kinetic constants for the bisubstrate reaction, as well as for allosteric inhibition and activation, were applied to Eq. (1), Eq. (2) and Eq. (5), respectively. The modeled $VNH_4^+$, considering a bi-bi random mechanism (Eq. 1), was plotted together with *in vivo* $RNH_4^+$ in Fig. 6a. Although modeled values underestimated actual ones, the trends for both treatments and organisms were accurately predicted. Accordingly, the relationship between modeled $VNH_4^+$ and measured $RNH_4^+$ yielded a much better correlation ($r^2 = 0.79$) than that obtained when using fixed GDH/$RNH_4^+$ ratios to estimate actual $RNH_4^+$ from GDH activities (Fig. 7). Furthermore, the percentages of either allosteric activation or inhibition are presented in Fig. 6b. Each effect resulted from the difference between the $VNH_4^+$ calculated at 0 mM of any effector and the $VNH_4^+$ at the actual effector concentration at any point throughout the time course. The main effects were found under well-fed conditions, either at $t_0$ or during re-feeding. Nevertheless, the magnitude of both inhibition and, more particularly, activation was significantly greater in *B. plicatilis* due to higher intracellular GTP and ADP concentrations (Fig. 5).

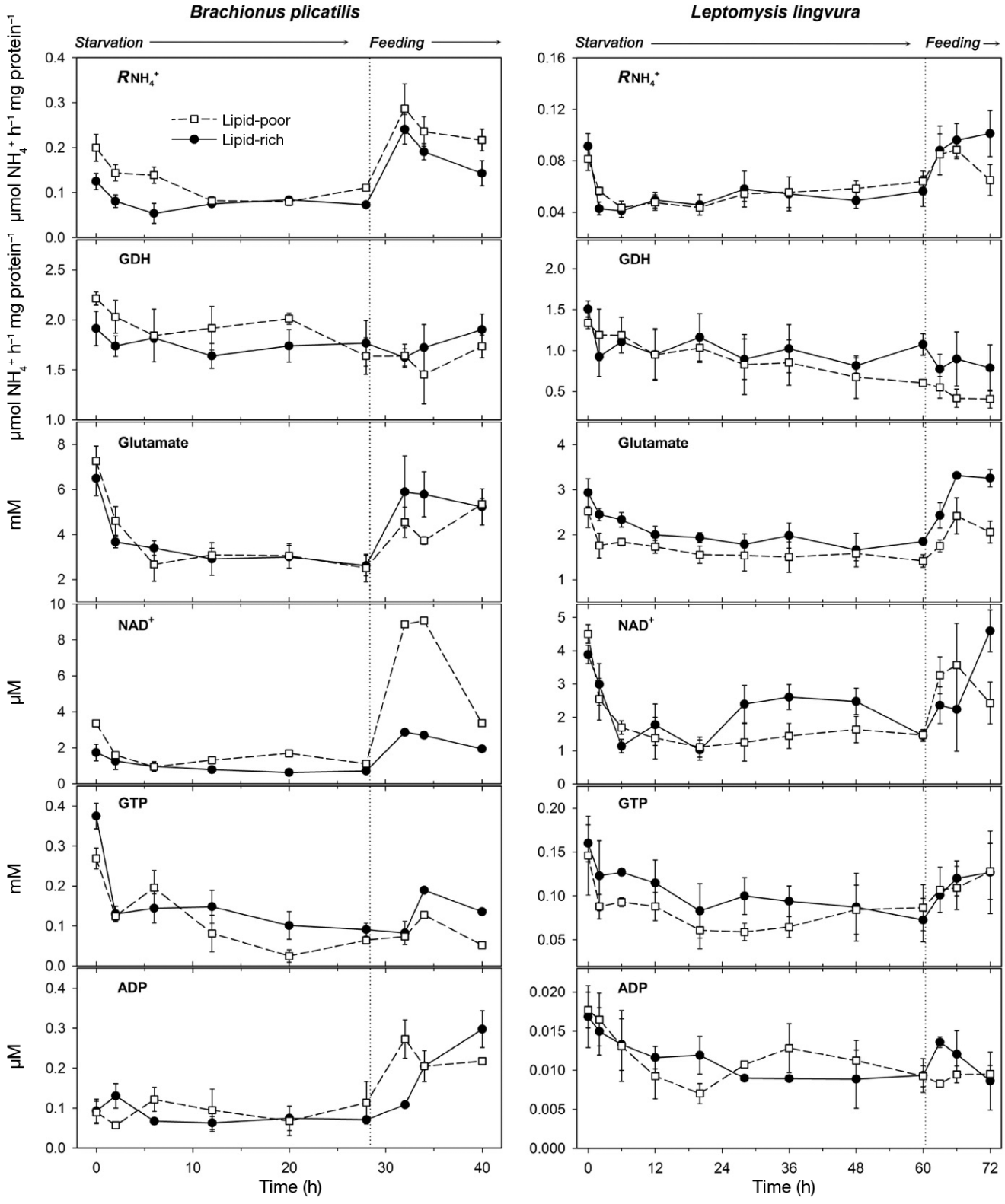


Fig. 5. Time profiles of $RNH_4^+$ and GDH activity (both standardized by protein content), as well as of intracellular metabolite concentrations (glutamate, $NAD^+$, GTP and ADP), for both *Brachionus plicatilis* and *Leptomysis lingvura* during starvation and after re-feeding, fed on lipid-rich and lipid-poor diets. Vertical dotted lines indicate the times at which organisms were re-fed. Error bars: 95% confidence intervals

Table 3. Kinetic constants for GDH in well-fed and starved rotifers (*Brachionus plicatilis*) and mysids (*Leptomysis lingvura*). Values are mean ± SD of n replicates. $V_{max}$: maximum velocity; $K_m$: half-saturation Michaelis constant; $K_{ia}$: enzyme substrate dissociation constant when either glutamate (Glu) or $NAD^+$ are the variable substrates, $K_i$: the inhibition constant when GTP is the variable substrate; $K_a$: the activation constant when ADP is the variable substrate. α and β are kinetic parameters for either the inhibition or activation. Eq.: equation used to fit the data

| | n | Variable substrate | Cosubstrate | $V_{max}$ (μmol $NH_4^+$ mg protein$^{-1}$ h$^{-1}$) | $K_m$ (mM) | $K_{ia}$, $K_i$, $K_a$ (mM) | α | β | Eq. |
|---|---|---|---|---|---|---|---|---|---|
| ***B. plicatilis*** | | | | | | | | | |
| Well-fed | 3 | Glu | $NAD^+$ (0.05–2 mM) | 1.61 ± 0.43 | 0.12 ± 0.01 | 14.75 ± 1.70 | – | – | 1 |
| | | $NAD^+$ | Glu (0.2–60 mM) | | 0.016 ± 0.007 | 0.85 ± 0.21 | – | – | 1 |
| | 3 | GTP | Glu (0.2–60 mM)[a] | 2.01 ± 0.36 | 0.37 ± 0.25[c] | $5.8 \times 10^{-4}$ ± $3.0 \times 10^{-4}$ | 2.05 ± 1.19 | 0.03 ± 0.01 | 2 |
| | 3 | ADP | Glu (0.2–60 mM)[a,b] | 0.078 ± 0.001 | 2.35 ± 1.20[c] | 4.10 ± 2.88 | 0.41 ± 0.19 | 29.98 ± 4.27 | 5 |
| Starved | 3 | Glu | $NAD^+$ (0.05–2 mM) | 1.39 ± 0.58 | 0.49 ± 0.14 | 26.53 ± 1.64 | – | – | 1 |
| | | $NAD^+$ | Glu (0.2–60 mM) | | 0.009 ± 0.003 | 0.67 ± 0.22 | – | – | 1 |
| | 4 | GTP | Glu (0.2–60 mM)[a] | 1.51 ± 0.62 | 1.07 ± 0.54[c] | $6.0 \times 10^{-4}$ ± $1.1 \times 10^{-4}$ | 4.13 ± 2.20 | 0.04 ± 0.02 | 2 |
| | 3 | ADP | Glu (0.2–60 mM)[a,b] | 0.084 ± 0.002 | 6.59 ± 3.92[c] | 3.55 ± 1.13 | 0.23 ± 0.01 | 11.69 ± 4.31 | 5 |
| ***L. lingvura*** | | | | | | | | | |
| Well-fed | 3 | Glu | $NAD^+$ (0.05–2 mM) | 1.77 ± 0.61 | 2.14 ± 0.23 | 7.72 ± 3.49 | – | – | 1 |
| | | $NAD^+$ | Glu (0.2–60 mM) | | 0.018 ± 0.006 | 0.44 ± 0.22 | – | – | 1 |
| | 3 | GTP | Glu (0.2–60 mM)[a] | 1.29 ± 0.20 | 1.39 ± 0.88[c] | $2.0 \times 10^{-3}$ ± $0.6 \times 10^{-3}$ | 2.50 ± 0.52 | 0.12 ± 0.02 | 2 |
| | 3 | ADP | Glu (0.2–60 mM)[a,b] | 0.34 ± 0.04 | 6.16 ± 1.85[c] | 0.70 ± 0.25 | 0.24 ± 0.01 | 3.16 ± 0.22 | 5 |
| Starved | 5 | Glu | $NAD^+$ (0.05–2 mM) | 1.02 ± 0.50 | 2.88 ± 0.32 | 14.52 ± 3.36 | – | – | 1 |
| | | $NAD^+$ | Glu (0.2–60 mM) | | 0.025 ± 0.005 | 0.73 ± 0.18 | – | – | 1 |
| | 4 | GTP | Glu (0.2–60 mM)[a] | 0.98 ± 0.49 | 2.06 ± 0.11[c] | $1.7 \times 10^{-3}$ ± $0.9 \times 10^{-3}$ | 5.04 ± 2.92 | 0.16 ± 0.06 | 2 |
| | 6 | ADP | Glu (0.2–60 mM)[a,b] | 0.34 ± 0.07 | 6.91 ± 2.23[c] | 5.76 ± 3.43 | 0.31 ± 0.24 | 4.63 ± 2.11 | 5 |

[a]All analyses were done at saturating levels of $NAD^+$ (1.2 mM); [b]These analyses consider $V_{max}$ and $K_{Glu}$ at 0 mM of ADP (i.e. without activation)
[c]Corresponding to the apparent $K_{Glu}$

## DISCUSSION

### Effect of diet on the $NH_4^+$ excretory metabolism

$NH_4^+$ production by zooplankton is recognized as a crucial process for nitrogen regeneration in the marine environment (Bronk & Steinberg 2008). However, despite its ecological significance, the biochemical mechanisms that govern the synthesis of $NH_4^+$ in marine heterotrophs have been poorly elucidated. There are basically 2 ways in which a metabolic rate is controlled during food shortage. On the one hand, enzyme concentration may vary according to food quantity; on the other hand, it may be regulated by intracellular metabolites. It is reasonable to presume that the earlier mechanism becomes more important in the long-term, as there would be no reason to maintain an excess of enzyme. But short-term, as is the case in the experiments presented here, substrate regulation of GDH activity may have certain advantages. Although the actual enzyme reaction rates may be difficult to determine from *in vitro* kinetic measurements due to cellular compartimentalization, metabolic channeling and competing reactions (Berges & Mulholland 2008), their study should provide useful information about regulatory patterns and biochemical adaptability in the face of environmental changes. This could be particularly interesting in highly variable ecosystems, where the use of a constant GDH/$R NH_4^+$ ratio may yield large errors in the appraisal of zooplankton $NH_4^+$ excretion (e.g. Hernández-León & Torres 1997). In fact, shifts in food availability have been found to generate fluctuations over an order of magnitude in the relationship between GDH activities and $R NH_4^+$ (Park 1986, Fernández-Urruzola et al. 2011), mainly because enzymatic rates were less responsive to the nutritional condition.

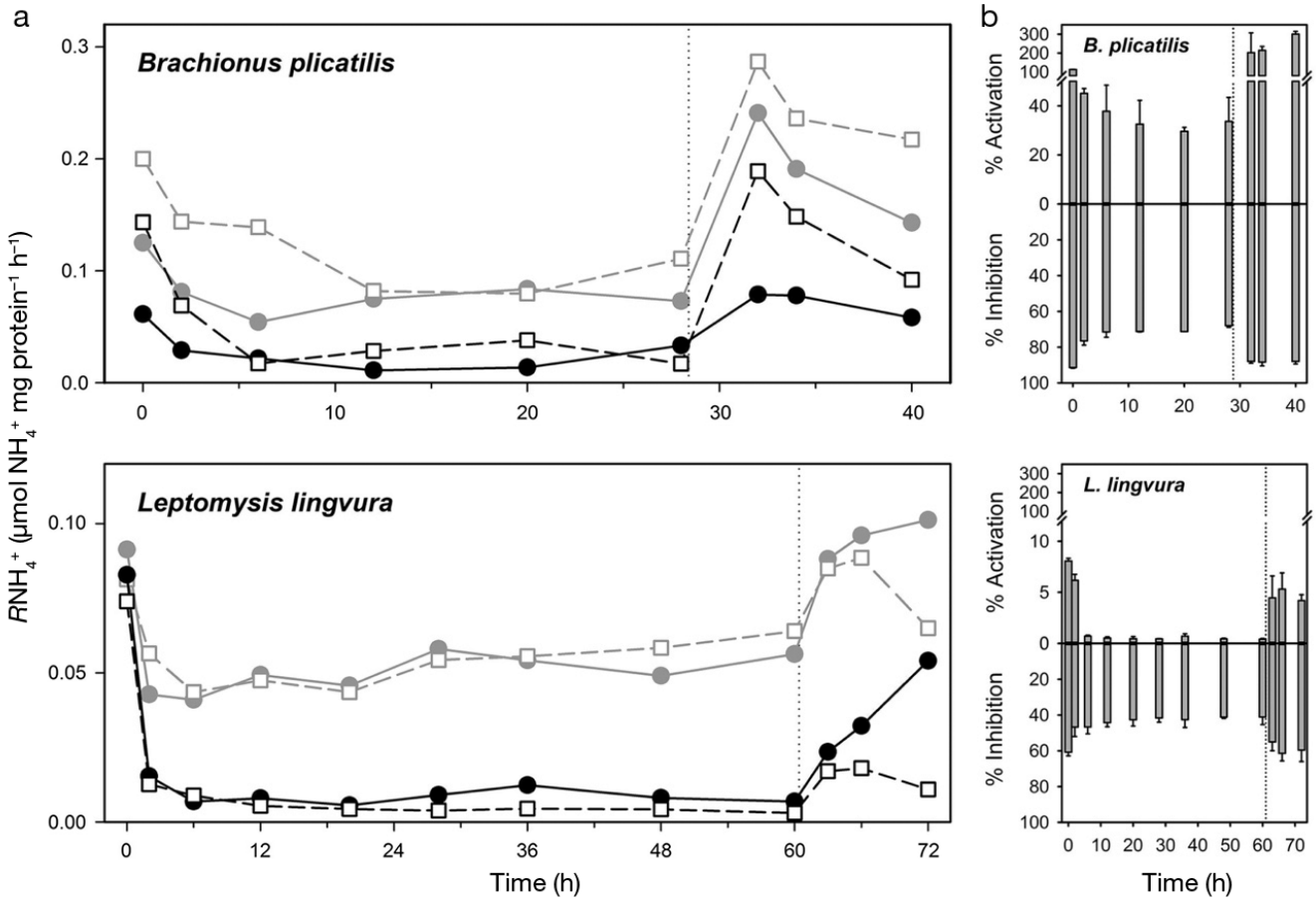


Fig. 6. *Brachionus plicatilis* and *Leptomysis lingvura*. (a) Modeled $R\mathrm{NH_4^+}$ ($V\mathrm{NH_4^+}$) after applying Eq. (1) at each sampling time during starvation experiments, in both lipid-rich (solid circles) and lipid-poor (open squares) treatments (black). The measured $R\mathrm{NH_4^+}$ is also presented for comparison (grey). Vertical dotted lines indicate the times at which organisms were re-fed. (b) Percentages of both inhibition and activation due to GTP and ADP molecules, calculated by applying the kinetic constants given in Table 3, using Eqs. (2) and (5), respectively. Both inhibition and activation were estimated as the difference between $V\mathrm{NH_4^+}$ at zero effector (and at the actual concentration of glutamate), which is represented by the horizontal line at 0%, and $V\mathrm{NH_4^+}$ at the actual effector concentration (and at the actual concentration of glutamate) at each sampling time. Note that the scales (in percent) for inhibition and activation are different

One factor that determines the amount of $\mathrm{NH_4^+}$ being excreted by zooplankton is the food ingested for assimilation (Miller & Roman 2008). The ratio between carbon and nitrogen contents in food influences the catabolism of nitrogenous compounds in zooplankton, meaning the higher the C/N ratio, the lower nitrogen release will be. In the rotifer case study, we show that food quality may indeed have an effect on $R\mathrm{NH_4^+}$ (Table 2)—as great as food availability (Fig. 5). This observation concurs with previous studies on a marine copepod that excreted more $\mathrm{NH_4^+}$ while being fed a carnivorous than a herbivorous diet (Saba et al. 2009). In this sense, prey, other than phytoplankton cells, would be metabolically beneficial, as nitrogen is assimilated more efficiently (Tang & Dam 1999). Despite the fact that *Nannochloropsis* sp. has a higher nutritional value, due to its higher polyunsaturated fatty acid content, than dry yeast (Tamaru et al. 1993), the latter contains more protein and little structural carbon, which increases assimilation efficiency. Since nitrogen comes exclusively from nitrogenous compounds, rotifers grown on yeast were expected to excrete more $\mathrm{NH_4^+}$. Such differences were not found in mysids, most likely because both heterotrophic diets were similar to each other at the protein level. GDH activities resembled $R\mathrm{NH_4^+}$ values, so the differences in GDH/$R\mathrm{NH_4^+}$ ratios were barely significant between treatments (Table 2). These differences were most noteable between taxonomic groups, so that the ratio peaked in mysids because of a lower mass-specific $R\mathrm{NH_4^+}$. Indeed, the trend for excretion rates to increase with decreasing body size is well known (Steinberg & Saba 2008). The distinct food qualities were also re-

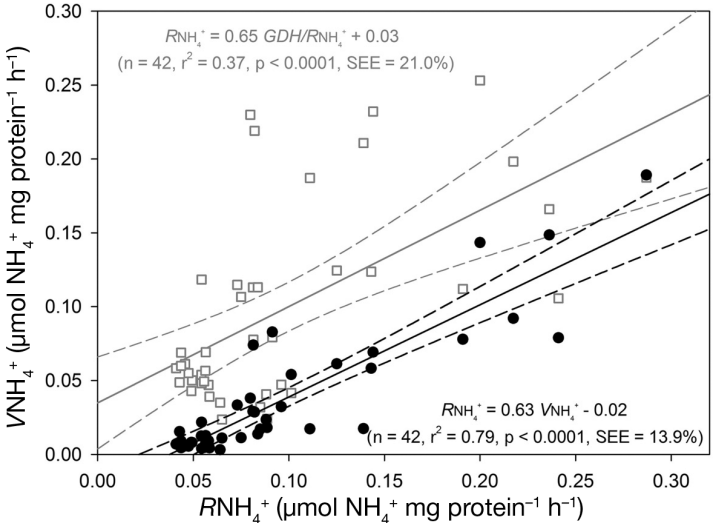


Fig. 7. Relationship between $VNH_4^+$ and $RNH_4^+$ measured during starvation experiments (●). The relationship between $RNH_4^+$ calculated from the GDH activities shown in Fig. 5 after applying the GDH/$RNH_4^+$ factors given in Table 2 (*y*-axis) and the measured $RNH_4^+$ (*x*-axis) is also presented (□). Dashed lines: 95% confidence intervals

flected in the $RO_2/RNH_4^+$ ratio, which is an index of metabolism (Mayzaud & Conover 1988). Thus, the lipid-rich diet in both organisms resulted in higher $RO_2/RNH_4^+$ values, especially in *Brachionus plicatilis*, where the $RO_2/RNH_4^+$ almost doubled (15.4) that for the lipid-poor treatment (8.8). According to the theoretical computations given in Mayzaud & Conover (1988), the diet based on the microalga *Nannochloropsis* sp. would induce more lipidic catabolism in rotifers, whereas all other diets, even that based on enriched *Artemia*, would promote pure protein catabolism in zooplankters. All these metabolic shifts according to the type of food barely affected the internal pool of metabolites.

### Kinetics of GDH during starvation

The metabolic response to feeding regime was almost immediate for both rotifers and mysids. The physiological and biochemical adjustments we observed align with previous studies on species of marine zooplankton that show a sharp decrease of either $RO_2$ or $RNH_4^+$ to a basal metabolism after ca. 6–8 h of starvation (Mayzaud 1976, Kiørboe et al. 1985). Similar changes in biochemical composition (in terms of carbon and nitrogen) were also observed by Mayzaud (1976). Irrespective of the diet used to grow zooplankters, here $RNH_4^+$ decreased about 2- to 3-fold within a few hours after food deprivation, and was rapidly restored to (or even surpassed) the original values of well-fed organisms when re-fed (Fig. 5). However, GDH activities followed a different pattern. In general, enzyme reaction rates are expected to vary more slowly and experience a certain delay compared to physiological rates (Bamstedt 1980). This has already been confirmed in starved *Leptomysis lingvura* for both GDH and ETS activities during a similar time course of starvation (Fernández-Urruzola et al. 2011, Herrera et al. 2011). This is reasonable short-term, because it is energetically most efficient to maintain constant enzymes levels in order to exploit resources when sudden changes in food abundance occur. Nevertheless, the maintenance of GDH activities will also depend on energy expenditure and the biochemical reserves that are available. In fact, those organisms grown on lipid-rich diets maintained their GDH activity at a relatively constant level compared to those organisms grown on a lipid-poor diet. Assuming similar energy requirements between treatments, the difference in their enzyme levels may be explained by the substrate that was being oxidized for energy production. Although lipid reserves are preferably used for basal metabolism during starvation (Bamstedt & Holt 1978), when exhausted, the hydrolysis of proteins would commence. This may result in an increase in protein breakdown and the metabolic oxidation of amino acids such as Glu in the lipid-poor treatments (Fig. 5). Furthermore, this biochemical pathway could be more relevant in *B. plicatilis*, as rotifers often have lower lipid stores than crustacean zooplankton.

Nevertheless, most of the metabolites varied in parallel with $RNH_4^+$ in both organisms, peaking during well-fed conditions. Similar trends according to fluctuations in the food environment have been described for the internal pool of Glu (Aragaõ et al. 2004) and $NAD^+$ (Osma et al. 2016) in small marine heterotrophs. This argues for a regulation mechanism via intracellular substrates, which would provide a nearly instantaneous fine-tuned adjustment of enzyme activity. GTP, in turn, is closely related to the energy charge, and, as such, reduced TCA cycle activity resulted in low levels of GTP during starvation. Since GTP is directly involved in cellular biosynthesis (Karl 1978), its decrease under food deprivation conditions reinforces the assumption that free amino acids are being metabolized for energy production.

Because of the simplicity of the single-substrate Michaelis-Menten equation, most biochemical research on marine organisms has used it to calculate

the half-saturation Michaelis constant ($K_m$) for every substrate of GDH (Bidigare & King 1981, Park 1986, Park et al. 1986, Fernández-Urruzola et al. 2011). However, a more extensive examination of GDH kinetics is needed to derive other related constants, such as the dissociation constant ($K_{ia}$), which requires bisubstrate enzyme kinetic studies. Due to their complexity (see Fig. 2), a lack of such determinations exist in marine literature, as they have only been estimated on the GDH of bovine liver (e.g. Barton & Fisher 1971). In the present study, $K_{Glu}$ calculated from bisubstrate analyses ranged from a low of 0.12 mM in rotifers to a high of 2.88 mM in mysids (Table 3). These values are slightly lower than those estimated in marine zooplankton according to a monosubstrate approach (ranging from 2.6 to 14.4 mM). The same occurs with $K_{NAD}$, which varied within a range (0.009–0.025 mM) much lower than the value (0.44 mM) reported in Fernández-Urruzola et al. (2011). A significantly lower $K_{NAD}$ as compared to $K_{Glu}$ suggests that GDH has a higher affinity for $NAD^+$ than it has for Glu; therefore, this pyridine nucleotide may be critical in regulating the enzyme reaction rate. Nevertheless, it has been shown that dicarboxylic substrates such as Glu enhance the affinity of $NAD^+$ by synergism to form ternary complexes (Rife & Cleland 1980). On the other hand, our calculations showed differences in the $K_m$ between organisms, as well as between feeding regimes, even though they were larger in the former case. This is not surprising, as several structures of GDH have been described across different phyla (Benachenhou-Lahfa et al. 1993), and a number of inducible isozymes that correlate with the nutritional condition can be present in a single species (Srivastava & Singh 1987). Regardless of such changes in kinetic constants, $K_{ia}$ values were, in all cases, higher than $K_m$ values (for Glu or $NAD^+$). Visually, this can be inferred from Fig. 2a, as the intersection point between the straight lines in the primary plot occurs above the abcissa. A higher $K_{ia}$ results in $K_m/K_{ia} < 1$, which means that the binding of one substrate to the active site increases the affinity for the other (Leskovac 2003).

However, these kinetics are complicated by allosteric modulation. The reaction rate of GDH can either be inhibited or stimulated by several molecules, among which the most important are the purine nucleotides (Frieden & Colman 1967). While GTP molecules are potent inhibitors of Glu deamination by increasing the binding affinity of the product, the ADP molecules act in an opposite manner facilitating $NH_4^+$ release. Their effects on both $K_{Glu}$ (considering Glu as the first binding substrate) and $V_{max}$ are determined by the factors α and β, respectively. Here, in the inhibition case study with GTP, α varied between 1 and ∞ and β varied between 0 and 1, which argues for hyperbolic mixed-type inhibition (Segel 1993). This means that both enzyme (E) and enzyme-inhibitor (EI) complexes bind to the substrate (S), but with different affinities. Although at different rates, both ES complex and enzyme-substrate-inhibitor (ESI) complex form products; therefore, an infinite concentration of inhibitor would not reduce the reaction velocity to zero. A similar concept, but applied in the opposite direction, should be applicable for activation with ADP. In the absence of an activator, $K_{Glu}$ increases significantly (see Table 3), in other words, the enzyme reduces its affinity for the substrate. In fact, when adding ADP to the standard assay in order to avoid any inhibition effect, what we really calculate are the apparent Michaelis kinetic parameters, $\alpha K_m$ and $\beta V_{max}$.

The benefits of using an enzyme kinetic model have already been shown for several key processes that are involved in respiratory metabolism (Packard et al. 1996, Roy & Packard 2001, Aguiar-González et al. 2012). Here, we used a similar theoretical concept to predict the velocity of $NH_4^+$ production in zooplankton, by applying the apparent $V_{max}$, the kinetic constants and the intracellular levels of Glu and $NAD^+$ in a first-principles-based equation (Eq. 1). This approach yields a mechanistic understanding of $NH_4^+$ excretion. The predicted $VNH_4^+$ along the starvation time course resembled the $RNH_4^+$ patterns measured in both rotifers and mysids reasonably well (Fig. 6a). However, it is noteable that $VNH_4^+$ underestimated the actual $RNH_4^+$, especially in the mysid case study. This may partially be due to conservative estimates of the intracellular levels of metabolites on a molar basis, as the general equation used for calculating mysid biovolume was obtained from zooplankters <5 mm (Alcaraz et al. 2003). Larger zooplankton would likely result in a lower volume per unit biomass. Furthermore, in eukaryotic cells, GDH is known to be mainly located in the mitochondria (Frigerio et al. 2008), so more precise determination of the mitochondrial matrix pool of substrates would make $VNH_4^+$ and $RNH_4^+$ more alike. In fact, GDH has been found to use the Glu available in close proximity to the reactive site, which comes from the deamidation by glutaminase of transported glutamine (Schoolwerth & LaNoue 1980). Nevertheless, none of these methodological constraints affect the patterns of $VNH_4^+$, but they could affect its magnitude. Still, this constraint could be solved through

calibration. The modeled $V\mathrm{NH_4^+}$ was clearly more successful in predicting the shape of $R\mathrm{NH_4^+}$ than were typical estimations from GDH activities (Fig. 7), even though 4 empirically determined GDH/$R\mathrm{NH_4^+}$ ratios for each organism and food treatment (Table 2) were applied to approximate the actual $R\mathrm{NH_4^+}$ from GDH measurements. Nevertheless, we can see from comparing this modeling effort with our attempts to calculate oceanic $R\mathrm{NH_4^+}$ from open-ocean GDH measurements and a general GDH/$R\mathrm{NH_4^+}$ factor that the enzyme kinetic model is a step in the right direction. Understanding how the effectors interact with each other and modulate $V\mathrm{NH_4^+}$ in bisubstrate kinetics is still a challenge. In the most simple case of monosubstrate kinetics (Eqs. 2 & 5), we have demonstrated that allosteric regulation, either for activation or inhibition, is more important during well-fed conditions (Fig. 6b). This concurs with the findings of Park et al. (1986), who suggested a greater inhibitory effect by GTP under high chlorophyll *a* situations. In spite of these challenges, we conclude that the use of the model's algorithm based on Michaelis-Menten substrate kinetics (Eq. 1) promises to provide better estimates of $R\mathrm{NH_4^+}$ in a changing environment.

## CONCLUSIONS

Zooplankton $\mathrm{NH_4^+}$ excretion constitutes an outstanding source of nitrogen that needs to be considered in the assessment of nutrient fluxes within the marine environment. Increased knowledge of the biochemical mechanisms that regulate the velocity of the GDH reaction will allow improvement of the appraisal of this metabolic process and, hence, the derivation of more precise conclusions about their role in biogeochemical cycles. Here we successfully applied enzyme kinetics to model $R\mathrm{NH_4^+}$ in 2 species of zooplankton. This introduces new insights in the study of $\mathrm{NH_4^+}$ excretion from *in vitro* enzymology, increasing the reliability of calculated $R\mathrm{NH_4^+}$ values under variable trophic situations, and establishes a baseline for future research of more complex GDH kinetics. In fact, this work does not pretend to be an extensive enzyme-kinetics binding study, but a relatively simple modeling exercise using the principles of enzymology to calculate the most basic kinetic constants in the control mechanisms of GDH. A more complex model involving other factors involved in enzyme reactions could have been constructed (Wells et al. 1977), but we have applied Ockham's razor (Ariew 1976) and used a simple model based on substrate activation. Had we done otherwise, the complexity would have been too costly or even impossible to accomplish experimentally. Still, our results indicate that, even in metazoans, simple kinetics can predict patterns of physiological rates ($R\mathrm{NH_4^+}$ in our case study) in a changing food environment, which reinforces the utility of these models in the study of zooplankton metabolism. Further research on metabolite fluctuations at the mitochondrial level would likely improve the kinetic model's calculations of the actual steady-state velocity of $\mathrm{NH_4^+}$ production.

*Acknowledgements*. We thank C. M. Hernández and D. López from the aquaculture research group (ULPGC) for providing us with strains of *Brachionus plicatilis* and *Nannochloropsis oculata*, as well as with helpful advice on setting up cultures. We are also grateful to J. J. Santana-Rodríguez for kindly lending us the equipment required to perform UHPLC analyses, and acknowledge 2 anonymous reviewers for their helpful comments on this manuscript. Funding was provided, in part, by the BIOMBA project (CTM2012-32729/MAR) and by the Innova Canarias 2020 program (Fundación Universitaria de Las Palmas), granted to M.G. and I.F.-U., respectively. I.F.-U. and N.O. were supported by postgraduate grants from the Formation and Perfection of the Researcher Personal Program from the Basque Government. T.T.P. was largely supported by TIAA-CREF and Social Security (USA).

## LITERATURE CITED

Aguiar-González B, Packard TT, Berdalet E, Roy S, Gómez M (2012) Respiration predicted from an enzyme kinetic model and the metabolic theory of ecology in two species of marine bacteria. J Exp Mar Biol Ecol 412:1–12

Alcaraz M, Saiz E, Calbet A, Trepat I (2003) Estimating zooplankton biomass through image analysis. Mar Biol 143: 307–315

Aragaõ C, Conceição LEC, Dinis MT, Fyhn HJ (2004) Aminoacid pools of rotifers and *Artemia* under different conditions: nutritional implications for fish larvae. Aquaculture 234:429–445

Ariew R (1976) Ockham's razor: a historical and philosophical analysis of Ockham's principle of parsimony. Pap Bibliogr Soc Am 70:101

Bamstedt U (1980) ETS activity as an estimator of respiratory rate of zooplankton populations. The significance of variations in environmental factors. J Exp Mar Biol Ecol 42: 267–283

Bamstedt U, Holt MR (1978) Experimental studies on the deep-water pelagic community of Korsfjorden, western Norway. Prey-size preference and feeding of *Euchaeta norvegica* (Gopepoda). Sarsia 63:225–236

Barton JS, Fisher JR (1971) Nonlinear kinetics of glutamate dehydrogenase. Studies with substrates — glutamate and nicotinamide-adenine dinucleotide. Biochemistry 10:577–585

Benachenhou-Lahfa N, Forterre P, Labedan B (1993) Evolution of glutamate dehydrogenase genes: evidence for two paralogous protein families and unusual branching

patterns of the archaebacteria in the universal tree of life. J Mol Evol 36:335–346

Berges JA, Mulholland MR (2008) Enzymes and nitrogen cycling. In: Carpenter EJ, Capone DG (eds) Nitrogen in the marine environment. Academic Press, London, p 1385–1444

Bidigare RR, King FD (1981) The measurement of glutamate dehydrogenase activity in *Praunus flexuosus* and its role in the regulation of ammonium excretion. Comp Biochem Physiol B 70:409–413

Bisswanger H (2008) Enzyme kinetics: principles and methods. Wiley-VCH, Weinheim

Bisswanger H (2011) Practical enzymology. Wiley-VCH, Weinheim

Boraas ME, Bennett WN (1988) Steady-state rotifer growth in a two-stage, computer-controlled turbidostat. J Plankton Res 10:1023–1038

Bronk DA, Steinberg DK (2008) Nitrogen regeneration. In: Carpenter EJ, Capone DG (eds) Nitrogen in the marine environment. Academic Press, London, p 385–467

Domingues PM, Fores R, Turk PE, Lee PG, Andrade JP (2000) Mysid culture: lowering costs with alternative diets. Aquacult Res 31:719–728

Engel PC, Dalziel K (1970) Kinetic studies of glutamate dehydrogenase: the reductive amination of 2-oxoglutarate. Biochem J 118:409–419

Fernández-Urruzola I (2016) Understanding the zooplankton ammonium excretion: from biogeochemical implications to intracellular regulatory mechanisms. PhD dissertation, University of Las Palmas de Gran Canaria, Las Palmas

Fernández-Urruzola I, Packard TT, Gómez M (2011) GDH activity and ammonium excretion in the marine mysid, *Leptomysis lingvura*: effects of age and starvation. J Exp Mar Biol Ecol 409:21–29

Fernández-Urruzola I, Osma N, Packard TT, Gómez M, Postel L (2014) Distribution of zooplankton biomass and potential metabolic activities across the northern Benguela upwelling system. J Mar Syst 140:138–149

Frieden C, Colman F (1967) Glutamate dehydrogenase concentration as a determinant in the effect of purine nucleotides on enzymatic activity. J Biol Chem 242: 1705–1715

Frigerio F, Casimir M, Carobbio S, Maechler P (2008) Tissue specificity of mitochondrial glutamate pathways and the control of metabolic homeostasis. Biochim Biophys Acta 1777:965–972

Guillard RRL (1975) Culture of phytoplankton for feeding marine invertebrates. In: Culture of marine invertebrate animals. Plenum Publishing Corp, New York, NY, p 108–132

Hans-Otto B, Michal G (1974) L-glutamate: determination with glutamate dehydrogenase, diaphorase, and tetrazolium salts. In: Bergmeyer HU (ed) Methods of enzymatic analysis. Verlag Chemie, Weinheim, p 1708–1713

Harrison WG (1992) Regeneration of nutrients. In: Falkowski PG, Woodhead AD (eds) Primary productivity and biogeochemical cycles in the sea. Plenum Press, New York, NY, p 385–409

Hernández-León S, Torres S (1997) The relationship between ammonia excretion and GDH activity in marine zooplankton. J Plankton Res 19:587–601

Herrera A, Packard T, Santana A, Gómez M (2011) Effect of starvation and feeding on respiratory metabolism in *Leptomysis lingvura* (G.O. Sars, 1866). J Exp Mar Biol Ecol 409:154–159

Holmes RM, Aminot A, Kérouel R, Hooker BA, Peterson BJ (1999) A simple and precise method for measuring ammonium in marine and freshwater ecosystems. Can J Fish Aquat Sci 56:1801–1808

Karl DM (1978) Occurrence and ecological significance of GTP in the ocean and in microbial cells. Appl Environ Microbiol 36:349–355

Kiørboe T, Møhlenberg F, Hamburger K (1985) Bioenergetics of the planktonic copepod *Acartia tonsa*: relation between feeding, egg production and respiration, and composition of specific dynamic action. Mar Ecol Prog Ser 26:85–97

Kirk KL (1997) Life-history responses to variable environments: starvation and reproduction in planktonic rotifers. Ecology 78:434–441

Leskovac V (2003) Comprehensive enzyme kinetics. Kluwer Academic Publishers, New York, NY

Lineweaver H, Burk D (1934) The determinations of enzyme dissociation constants. J Am Chem Soc 56:658–666

Lowry OH, Rosebrough NJ, Farr AL, Randall RJ (1951) Protein measurement with the Folin phenol reagent. J Biol Chem 193:265–275

Lubzens E, Gibson O, Zmora O, Sukenik A (1995) Potential advantages of frozen algae (*Nannochloropsis* sp.) for rotifer (*Brachionus plicatilis*) culture. Aquaculture 133: 295–309

Maldonado F, Packard TT, Gómez M (2012) Understanding tetrazolium reduction and the importance of substrates in measuring respiratory electron transport activity. J Exp Mar Biol Ecol 434-435:110–118

Mayzaud P (1976) Respiration and nitrogen excretion of zooplankton. IV. The influence of starvation on the metabolism and the biochemical composition of some species. Mar Biol 37:47–58

Mayzaud P, Conover RJ (1988) O:N atomic ratio as a tool to describe zooplankton metabolism. Mar Ecol Prog Ser 45: 289–302

Miller CA, Roman MR (2008) Effects of food nitrogen content and concentration on the forms of nitrogen excreted by the calanoid copepod, *Acartia tonsa.* J Exp Mar Biol Ecol 359:11–17

Osma N (2016) On the respiratory metabolism of marine plankton: its application in assessing carbon fluxes and the role of substrates in its biochemical control. PhD dissertation, University of Las Palmas de Gran Canaria, Las Palmas

Packard TT, Gómez M (2008) Exploring a first-principles-based model for zooplankton respiration. ICES J Mar Sci 65:371–378

Packard TT, Berdalet E, Blasco D, Roy SO and others (1996) Oxygen consumption in the marine bacterium *Pseudomonas nautica* predicted from ETS activity and bisubstrate enzyme kinetics. J Plankton Res 18:1819–1835

Packard TT, Blasco D, Estrada M (2004) Modeling physiological processes in plankton on enzyme kinetic principles. Sci Mar 68:49–56

Park YC (1986) Impact of starvation and feeding experiments on ammonium excretion and glutamate dehydrogenase activity of zooplankton. Kor Biochem J 19:251–256

Park YC, Carpenter EJ, Falkowski PG (1986) Ammonium excretion and glutamate dehydrogenase activity of zooplankton in Great South Bay, New York. J Plankton Res 8:489–503

Postel L, Fock H, Hagen W (2000) Biomass and abundance.

In: Harris RP, Wiebe PH, Lenz J, Skjoldal HR, Huntley M (eds) ICES zooplankton methodology manual. Academic Press, San Diego, CA, p 83–192

Regnault M (1987) Nitrogen excretion in marine and freshwater crustacea. Biol Rev Camb Philos Soc 62:1–24

Rife JE, Cleland WW (1980) Kinetic mechanism of glutamate dehydrogenase. Biochemistry 19:2321–2328

Roy SO, Packard TT (2001) $CO_2$ production rate predicted from isocitrate dehydrogenase activity, intracellular substrate concentrations and kinetic constants in the marine bacterium *Pseudomonas nautica*. Mar Biol 138:1251–1258

Rutter WJ (1967) Protein determination in embryos. In: Wilt FH, Wessels NV (eds) Methods in developmental biology. Academic Press, London, p 671–684

Saba GK, Steinberg DK, Bronk DA (2009) Effects of diet on release of dissolved organic and inorganic nutrients by the copepod *Acartia tonsa*. Mar Ecol Prog Ser 386:147–161

Schoolwerth AC, LaNoue KF (1980) The role of microcompartmentation in the regulation of glutamate metabolism by rat kidney mitochondria. J Biol Chem 255: 3403–3411

Segel IH (1993) Enzyme kinetics. Behaviour and analysis of rapid equilibrium and steady-state enzyme systems. John Wiley & Sons, New York, NY

Srivastava HS, Singh RP (1987) Role and regulation of L-glutamate dehydrogenase activity in higher plants. Phytochemistry 26:597–610

Steinberg DK, Saba GK (2008) Nitrogen consumption and metabolism in marine zooplankton. In: Carpenter EJ, Capone DG (eds) Nitrogen in the marine environment. Academic Press, London, p 1135–1196

Tamaru CS, Murashige R, Lee CS, Ako H, Sato V (1993) Rotifers fed various diets of baker's yeast and/or *Nannochloropsis oculata* and their effect on the growth and survival of striped mullet (*Mugil cephalus*) and milkfish (*Chanos chanos*) larvae. Aquaculture 110:361–372

Tang KW, Dam HG (1999) Limitation of zooplankton production: beyond stoichiometry. Oikos 84:537–542

Wagner TC, Scott MD (1994) Single extraction method for the spectrophotometric quantification of oxidized and reduced pyridine nucleotides in eritrocytes. Anal Biochem 222:417–426

Wells BD, Parks LA, Tam I, Fisher JR (1977) A kinetic model for glutamate dehydrogenase. J Theor Biol 66:81–93

*Editorial responsibility: Antonio Bode, A Coruña, Spain*

*Submitted: October 26, 2015; Accepted: March 17, 2016*
*Proofs received from author(s): May 11, 2016*